

# Influence of Soil and Structural Parameters on Liquefaction-Induced Settlement of Foundations



Zana Karimi, Zach Bullock, Shideh Dashti, Abbie Liel & Keith Porter

*Department of Civil, Environmental and Architectural Engineering – University of Colorado Boulder, Boulder, CO, USA*

## ABSTRACT

Large seismic deformations in liquefiable soils beneath shallow-founded structures have led to excessive damage and repair cost in previous earthquakes. The existing procedures for evaluating liquefaction-induced building settlement based on volumetric strains have repeatedly been shown as unreliable and inaccurate during previous case histories and physical model studies, as they ignore the key mechanisms of deformation near buildings. In this paper, we set the stage for a performance-based predictive approach to assess the permanent settlement of structures with mat foundations on liquefiable soils. Such an approach requires a robust database that account for the most important parameters controlling the main mechanisms of settlement. In a numerical parametric plan, the fully-coupled dynamic response of soil-foundation-structure systems is evaluated under a wide range of soil, structural, and ground motion characteristics. The primary goal is to identify the key predictors of foundation settlement and quantify their relative importance. The input parameters evaluated are: the building's height/width ratio; the foundation's bearing pressure and contact area; the liquefiable layer's relative density and thickness; and the earthquake motion's characteristics. Ground motions are selected from different tectonic environments, covering a wide range of intensity, duration, and frequency content. The numerical simulations involve fully-coupled, 3-dimensional, nonlinear dynamic analyses of the soil-foundation-structure system, which was previously validated using centrifuge experimental results. For the conditions considered, the key predictors of building settlement are identified as the relative density and thickness of the liquefiable layer followed by foundation contact area and bearing pressure. The structures' height/width ratio matters comparatively less. Most of the parameters become more influential with increasing the motion intensity and duration, and some become more or less influential when the relative density of the liquefiable layer increases. These analyses provide the database for developing future probabilistic predictive models to estimate the settlement of shallow-founded structures on liquefiable ground.

## 1 INTRODUCTION

Case studies from past earthquakes show that shallow-founded buildings and their surrounding lifelines, even those designed based on advanced regulations, may be prone to extensive damage due to soil liquefaction and its consequences. For example, buildings with shallow foundations suffered from extensive settlement, tilt, and lateral sliding during the 2010-2011 Christchurch series of earthquakes (Cubrinovski and McCahon 2012). Advancements in our understanding of the response of shallow-founded structures on liquefiable deposits have been achieved through past experimental and numerical studies, as well these case history observations. Yet, there are still no predictive models of building response on liquefiable ground that are mechanistically sound, and validated against case history and physical model studies. This limitation points to the need for a more robust procedure to estimate the performance of shallow-founded structures, which would take all of the significant controlling parameters affecting soil-foundation-structure interaction (SFSI) into account.

Existing methods for estimating settlement on liquefiable soils (e.g., Tokimatsu and Seed 1987; Ishihara and Yoshimine 1992) are primarily semi-empirical simplified procedures that ignore the presence of the superstructure and its interactions with the underlying soil.

In these procedures, soil response is assumed to be fully undrained during seismic loading, and free-field settlement is calculated based on post-liquefaction volumetric strains alone. Experimental and numerical studies have found not only that partial drainage occurs during (as well as after) cyclic loading, but also that settlement near shallow-founded structures is often dominated by shear type deformations (Dashti et al. 2010a,b; Karimi and Dashti 2015a,b 2016a). The seismic response of a soil-foundation-structure (SFS) system therefore is strongly influenced by the dynamic characteristics of the structure and ground motion as well as the structure's interaction with the underlying soil.

In this study, we seek to advance a performance-based framework for estimating the settlement of shallow-founded structures on liquefiable deposits. Any predictive model for a highly nonlinear SFSI problem requires robust simulations that are validated rigorously. Here, we present results from a numerical study to evaluate SFSI effects and changes in the seismic demand imposed on the foundation through a liquefiable soil deposit. We also use the results of the numerical parametric study to identify the structural and soil input parameters (IPs) or predictors that have the most significant influence on the average permanent foundation settlement of a single-degree-of-freedom (SDOF) building on liquefiable ground. In addition, the seismic demand at the foundation level is

compared with those at the free-field soil surface and at the elastic bedrock level through time-frequency domain analyses of the accelerations. This analysis helps to evaluate the relationship between the timing of liquefaction and changes in the frequency content and amplitude of free-field and foundation accelerations, which control the demand imposed on the superstructure and timing and rate of foundation settlement. The influence of each IP on the mechanisms contributing to foundation settlement is subsequently discussed in detail to identify the key predictors of settlement.

### 1.1 Numerical Simulation and Validation

For the numerical parametric study, the SFS system was modeled using 3-D fully-coupled nonlinear dynamic finite element analyses. Figure 1 presents the finite element mesh configuration of an example model. The pressure-dependent, multi-yield-surface, plasticity-based soil constitutive model (PDMY02) implemented in OpenSees by Elgamal et al. (2002) and Yang et al. (2003, 2008) was used to represent the nonlinear response of saturated sand. In this model, the yield criteria are defined by a number of open conical-shaped yield surfaces with the apex located at the origin of the principal stress space. This model uses a non-associative flow rule that produces volumetric dilation and contraction under shear deformation. In this model, no plastic change of volume takes place under a constant stress ratio, since the yield surfaces are open-ended. 8-node BrickUP elements were used to model the soil medium. The SDOF structure and its foundation were modeled with brick elements and elastic material properties to better represent the geometry and components of the structural models used in the centrifuge experiments

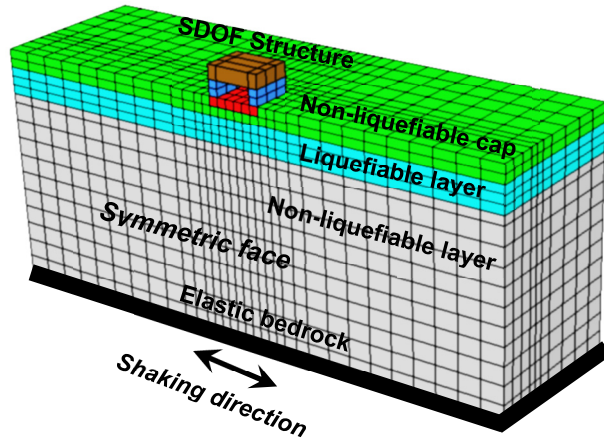


Figure 1. Finite element discretization of the SFS system.

The numerical model employed in this study was previously validated by Karimi and Dashti (2015a,b, 2016a) using centrifuge experiments of SDOF structures on layered liquefiable deposits that were conducted by Dashti et al. (2010a,b). Analyses were performed in 3-D to more accurately simulate the response of shallow-

founded structures on liquefiable ground and the 3D stress and drainage conditions. The temporal and spatial initiation of liquefaction triggering, softening followed by re-stiffening, and the resulting excess pore pressures, soil and structural accelerations, and displacements near the structure were evaluated in time-domain analyses, which compared well with experimental observations. Details of the numerical simulations, calibrated soil parameters, and validation results were discussed in detail by Karimi and Dashti (2015a,b, 2016a), and are not repeated here for brevity.

## 2 OVERVIEW OF NUMERICAL PARAMETRIC STUDY AND GROUND MOTION SELECTION

In an extensive numerical parametric study, the effects of a wide range of soil, structural, and ground motion IPs on average foundation settlement were assessed and quantified. These models consisted of SDOF shallow-founded structures on layered soil deposits including a single layer of liquefiable sand. The bedrock below the soil deposit was assumed to be elastic in the parametric studies (bedrock shear wave velocity,  $V_s=760$  m/s), as shown in Figure 1.

Seventy-four model configurations were simulated with variations in thickness ( $H_L = 2$  to 20 m) and relative density ( $D_{rL} = 30$  to 85%) of the liquefiable layer, the foundation contact pressure ( $q = 30$  to 190 kPa) and area ( $A = 30$  to 330  $m^2$ ), and the structure's height to width ratio ( $H/B = 0.25$  to 2.25, where direction of B is parallel to the direction of shaking). In the presented analyses, the depth to the shallow liquefiable layer was kept constant (2 m). Table 1 shows a summary of the model properties discussed in this paper. Other simulations were conducted to evaluate the influence of depth to liquefiable layer, overall thickness of the soil column, the presence of multiple liquefiable layers, as well as the inertial mass and fundamental period of the structure. Those results will be investigated in future publications. Further, although some of the parameters presented are likely to be highly correlated, each parameter is tested individually here to isolate its influence on average foundation settlement.

Table 1. Properties of the SFS systems considered in the numerical parametric study

Input Parameter (IP)	Value of IP
Liquefiable Layer Relative Density, $D_{rL}$ (%)	30, 40, 50, 60, 70, and 85
Liquefiable Layer Thickness, $H_L$ (m)	1, 2, 3, 4, 6, 8, 12, 14, 16, and 20
Building Height, $H/B$ ratio	0.25, 0.5, 0.75, 1.00, 1.25, 1.5, 1.75, 2.00, and 2.25
Foundation Bearing Pressure, $q$ (kPa)	30, 60, 90, 110, 130, 160, 190, and 220
Foundation Contact Area, $A$ ( $m^2$ )	30, 54, 85, 120, 165, 216, and 340

A suite of 150 ground motions, with earthquake moment magnitudes ( $M_w$ ) ranging from 4.5 to 9.0, closest site-to-source distance ( $R$ ) up to 400 km, and sites with  $V_{s,30}$  ranging from 760 to 2000 m/s to represent bedrock were applied to the elastic base of the numerical models. The recorded ground motions had peak ground accelerations (PGA) ranging from 7 to 1600  $\text{cm/s}^2$ , and cumulative absolute velocities (CAV) from 10 to 7000  $\text{cm/s}$ . The ground motions were selected from different tectonic environments to cover a wide range of intensity, duration, and frequency characteristics. Figure 2 shows the distribution of ground motion characteristics used as outcropping rock motions input to the numerical models. Each excitation was applied to the elastic bedrock through a force time history derived according to the ground motion velocity time histories and assumed properties of the bedrock (e.g., bedrock shear wave velocity and density), similar to the approach used by Zhang et al. (2008).

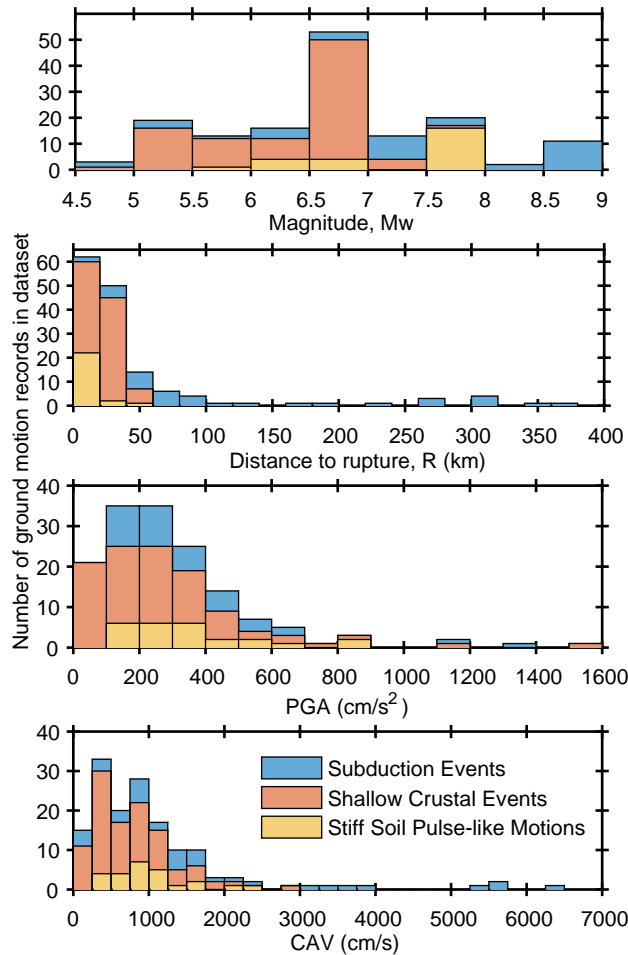


Figure 2. Input ground motion characteristics applied to the elastic bedrock in the numerical analyses.

### 3 RESULTS AND DISCUSSIONS

#### 3.1 Influence of Excess Pore Pressures on Foundation Acceleration and Settlement

Before evaluating the influence of various IPs on foundation settlement, it is insightful to mechanistically evaluate the relationship between the timing of excess pore pressure generation and liquefaction with SFSI effects and therefore the foundation's acceleration and settlement response. The change in the frequency content of acceleration in the far-field soil surface (FF) and foundation (FM) was evaluated in time using Stockwell transforms (Stockwell 1996) for a few representative models and ground motions, similar to the approach taken by Kramer et al. (2015).

Figure 3 shows the time history and Stockwell spectra of the base rock motion (BM), FF, and FM obtained from one model configuration and ground motion, as an example. In this model, the relative density, thickness of, and depth to the liquefiable layer were 50%, 3 m, and 2m, respectively. The input ground motion for this case had a PGA of 316  $\text{cm/s}^2$  (0.32 g) and a CAV of 1,501  $\text{cm/s}$ . Foundation settlement as well as excess pore water pressure time histories predicted in the middle of the liquefiable layer both in the far-field and under the foundation are plotted for comparison in Figure 4.

The dominant frequency content of the BM computed at the elastic bedrock ranged from 0.5 to 10 Hz. As excess pore water pressures developed within the liquefiable layer during shaking (Figure 4), the sand softened and reduced the seismic demand (amplitude of accelerations) transferred to the surface of the liquefiable layer. In the far-field, liquefaction (defined as  $r_u = u_e / \sigma_{v0} = 1.0$ , where  $u_e$  and  $\sigma_{v0}$  are excess pore pressure and initial vertical effective stress, respectively) was observed at  $t = 7-8$  s during this particular motion.

Under the center of the foundation, due to the influence of additional confining pressures, complete liquefaction ( $r_u = 1.0$ ) was never reached during this motion, even though large excess pore pressures were generated. This response affected the frequency content of the FF and FM motions. In the FF, the dominant frequency content reduced to approximately 1 Hz quickly after 7 to 8 s (Figure 3). A reduction in the overall frequency content of the FM acceleration was also observed, but higher frequencies were sustained for a longer portion of the ground motion. FM also contains frequency content above 10 Hz, which is due to SFSI effects. The foundation started to settle with the start of cyclic loading approximately linearly with time (Figure 4). This settlement continued until the end of shaking when the net excess pore pressures started to drop ( $t = 40$  s, in this case). Although the  $r_u$  value never reached unity under the foundation in this example (and most cases simulated), still large average permanent settlements of about 320 mm were predicted during this motion due to extensive softening. The significant drop in the foundation's settlement rate after the end of strong shaking also points to the importance of soil-structure interaction induced, shear-type, building ratcheting that occurs during seismic loading.

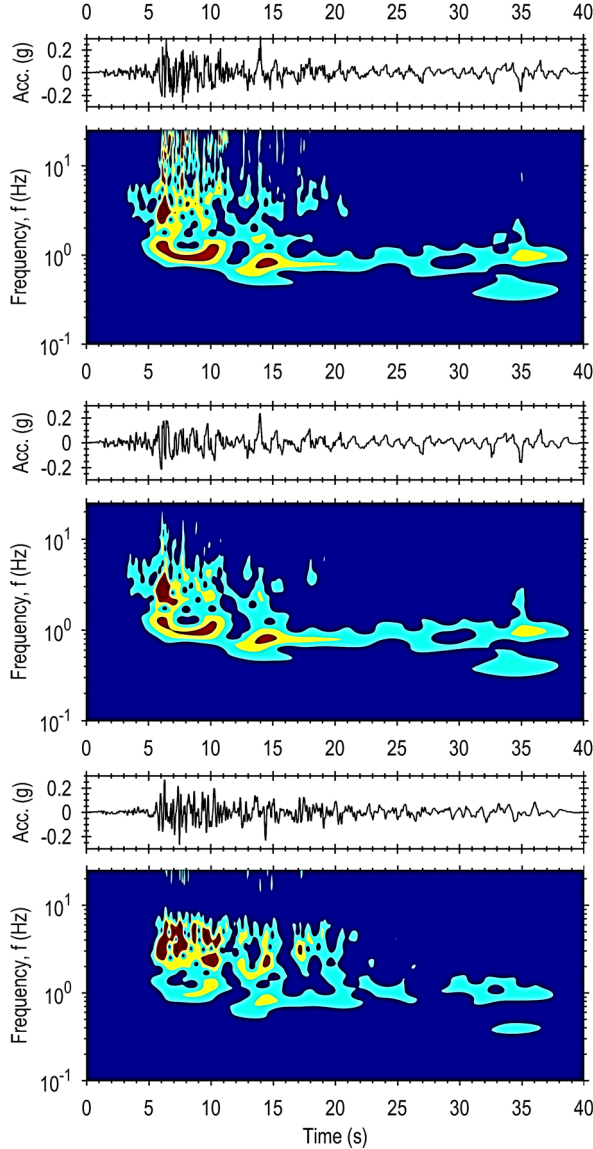


Figure 3. Time history and Stockwell spectrum of the ground motion accelerations recorded at the bedrock (BM), surface of the far-field (FF), and the foundation level (FM) in a single time-domain analysis of a representative SFS system.

### 3.2 Influence of Input Parameters on the Average Foundation Settlement

Karimi and Dashti (2016b, 2017), Dashti and Karimi (2017), and Karimi et al. (2017) showed that evolutionary ground motion intensity measures (IMs), such as CAV, are stronger predictors of average foundation settlement than traditional IMs that are based on a single peak value of acceleration or velocity (e.g., PGA or PGV). That study also showed that the uncertainty and variability in settlement predictions reduces when IMs are quantified based on the motion at the bedrock level (i.e., BM) compared to those in the far-field soil surface (FF) or at

the foundation level (FM). Therefore, here the results are plotted against CAV of the BM to evaluate the influence of other soil and structural IPs on liquefaction-induced foundation settlements. In the following figures, the results of numerical simulations are plotted for three different relative densities of the liquefiable layer ( $D_{rL}$ ) in each case: loose sand ( $D_{rL}=30\%$ ), medium-dense sand ( $D_{rL}=50\%$ ), and dense/non-liquefiable sand ( $D_{rL}=85\%$ ).

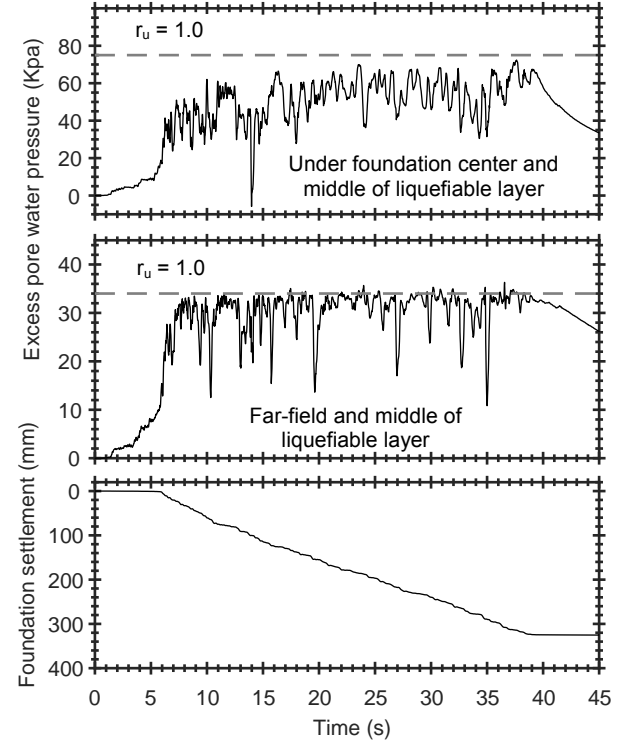


Figure 4. Excess pore water pressure time histories recorded in the middle of the liquefiable layer in the far-field or under the center of the foundation, along with the average foundation settlement time history in a single time-domain analysis of a representative SFS system.

Figure 5 shows the influence of the liquefiable layer thickness ( $H_L$ ) on average permanent foundation settlement. The results are presented for a loose ( $D_{rL}=30\%$ ) and medium-dense ( $D_{rL}=50\%$ ) liquefiable layers. For the loose and medium-dense cases, an increase in  $H_L$  up to about 8 to 10 m increased foundation settlements. For thicker layers, depending on the intensity of the ground motion, the settlements reached a plateau or decreased slightly.

In general, for a given soil-foundation-structure system, the amount of foundation settlement depends on the degree of soil softening (strength loss) and the seismic demand experienced by the foundation (FM); these factors control both volumetric and shear type displacements under the foundation. The potential for excess pore pressure generation and subsequent soil softening increases as  $H_L$  grows, due to a greater volume of looser soils generating large excess pore pressures.



However, at some level, increasing  $H_L$  no longer amplifies total shear type deformations in the foundation soil that tend to control building settlements. In fact, foundation settlement starts to slightly decrease at greater  $H_L$  beyond this threshold during strong levels of shaking. This reduction is due to further strength loss in the liquefiable soil and the reduction in the acceleration transferred to the foundation (FM) and superstructure, particularly at higher frequencies (as previously shown in Figure 3). The softened liquefiable layer acts as a base isolator, and with greater softening, it starts to reduce the FM and subsequent SSI-induced building ratcheting, the net effect of which is a slight reduction in foundation settlement.

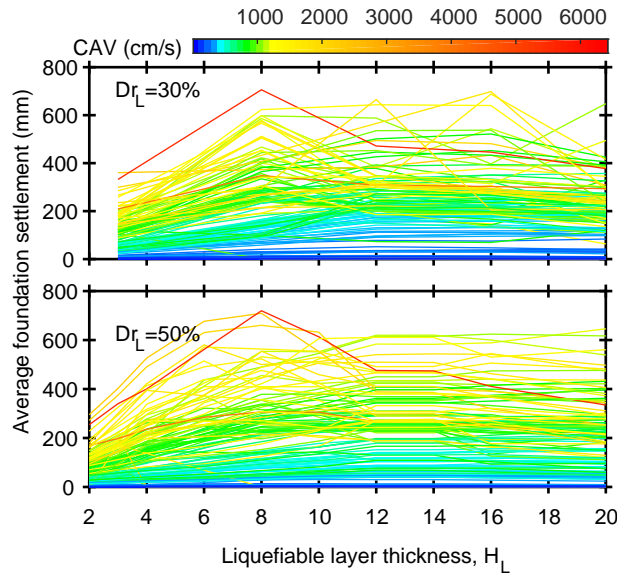


Figure 5. Influence of the liquefiable layer thickness on average permanent foundation settlements.

For the case of  $Dr_L=85\%$ , when the entire soil column below the cap layer is non-liquefiable or dense, foundation settlements of up to approximately 200 mm were computed under strong levels of shaking. This observation is important, indicating when densification techniques (i.e., increasing soil relative density) are considered to mitigate the consequences of liquefaction, seismic settlements may still be unacceptable under the foundation.

Figure 6 shows the influence of foundation contact pressure ( $q$ ) on its average settlement, when the thickness of the liquefiable layer is kept constant at 3m.

In general, with increasing  $q$ , the base shear stress applied to the softened soil and the subsequent shear or deviatoric settlements under the foundation amplify until they eventually reach a plateau, beyond which settlement does not appear to be sensitive to further increases in  $q$ . The sensitivity of the foundation settlement to  $q$  is greater for loose and medium dense sand layers, as compared to a dense condition. This sensitivity increases with greater shaking intensity for all soil relative densities.

Figure 7 shows the effects of foundation contact area ( $A$ ) on its average settlement. In this set of simulations,  $H_L$

and  $q$  are kept constant at 3m and 76 kPa, respectively. Importantly, the  $H/B$  ratio of the structure is also kept constant at 0.57.

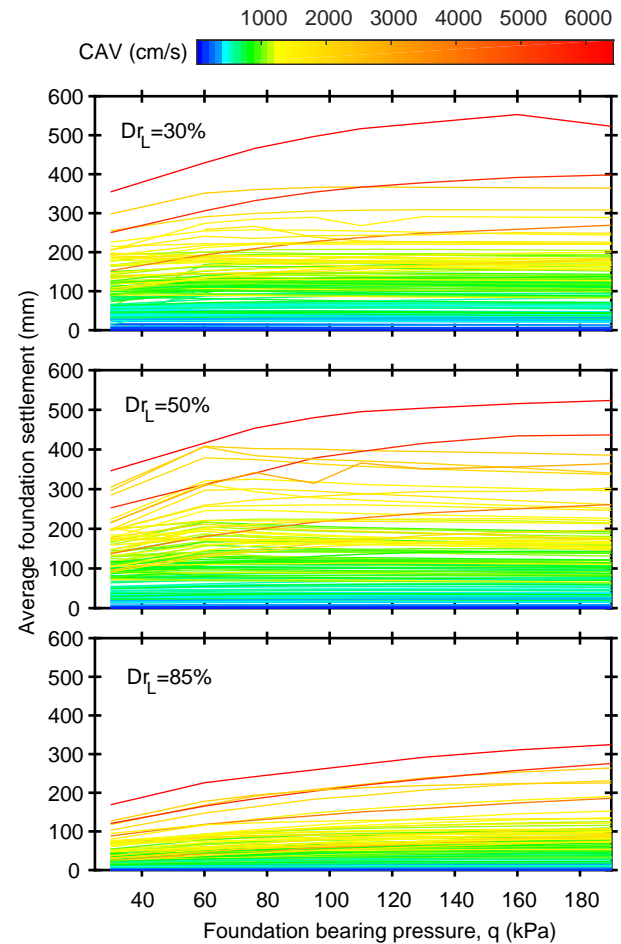


Figure 6. Influence of the foundation contact pressure on average permanent foundation settlements.

In general, larger  $A$  does not significantly impact the settlement, but this trend varies with shaking intensity and relative density. Increases in  $A$  alone result in larger bulbs of stress in the soil beneath the foundation, penetrating wider and deeper into the ground. Therefore, the confining pressure (or  $\sigma'_{v0}$ ) increases in a larger volume of soil underneath the foundation. This larger confinement increases the soil's resistance to liquefaction ( $r_u=1.0$ ) and strength loss, which would reduce shear type displacements under the foundation. However, under the same condition, greater net excess pore pressures could generate under the higher confinement during stronger levels of shaking (i.e., soil becomes more contractive). Furthermore, a larger foundation contact area elongates the drainage path, which in turn increases the potential for excess pore pressures to build up, reducing the rate of pore pressure dissipation underneath the foundation during shaking.

The net influence of these at times conflicting effects is the following trends with increasing foundation area ( $A$ ): for small to moderate levels of shaking, and for loose to medium-dense liquefiable soils, we observe a slight decrease in settlement (up to  $A$  of about  $100 \text{ m}^2$ ), after which increasing  $A$  does not appear influence settlement. This trend is due to the increased confinement and subsequent increase in resistance against strength loss, which reduces slightly the contribution of shear strains under the larger foundations. However, if the motion is strong enough to cause significant net excess pore pressure generation underneath the foundation, settlements can increase by up to 200%, when  $A$  approximately increased from 25 to  $340 \text{ m}^2$ , and they eventually reach a plateau. At stronger levels of shaking, significant strength loss can occur, while larger net pore pressures would amplify volumetric strains due to partial drainage. This trend is also observed in the dense layer during strong motions, since the increase in confinement increases the contraction tendency of the soil or its potential for large net excess pore pressure generation.

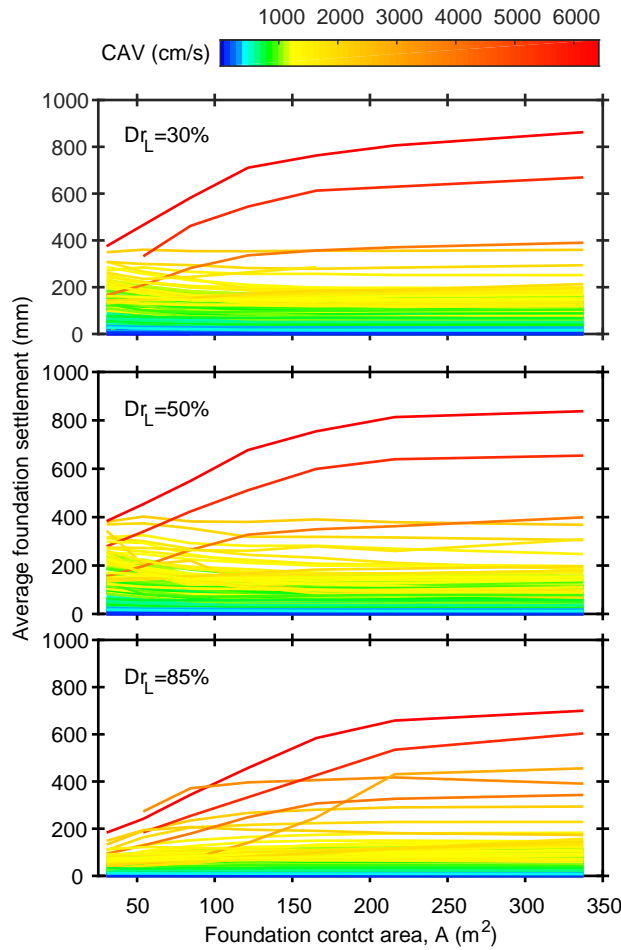


Figure 7. Influence of the foundation contact area on average permanent foundation settlements.

Lastly, Figure 8 shows the influence of structural height/width ratio ( $H/B$ ) on its average permanent settlement. In these models, the contact area and pressure were kept at  $54 \text{ m}^2$  and  $76 \text{ kPa}$ , respectively. Fixed base fundamental period of the SDOF structure was  $0.4 \text{ s}$  and kept constant (by adjusting lateral stiffness of columns) to only evaluate the influence of  $H/B$  ratio. For the cases considered in this study, increasing the  $H/B$  ratio alone increases foundation settlement only slightly, particularly for the stronger levels of shaking. This is due to the increased base moment and tendency for SSI-induced building ratcheting during cyclic loading. This influence was not significant without a simultaneous increase in building mass and contact pressure.  $H/B$ , however, was observed to more strongly correlate with permanent foundation rotation or tilt, which is not discussed in this paper.

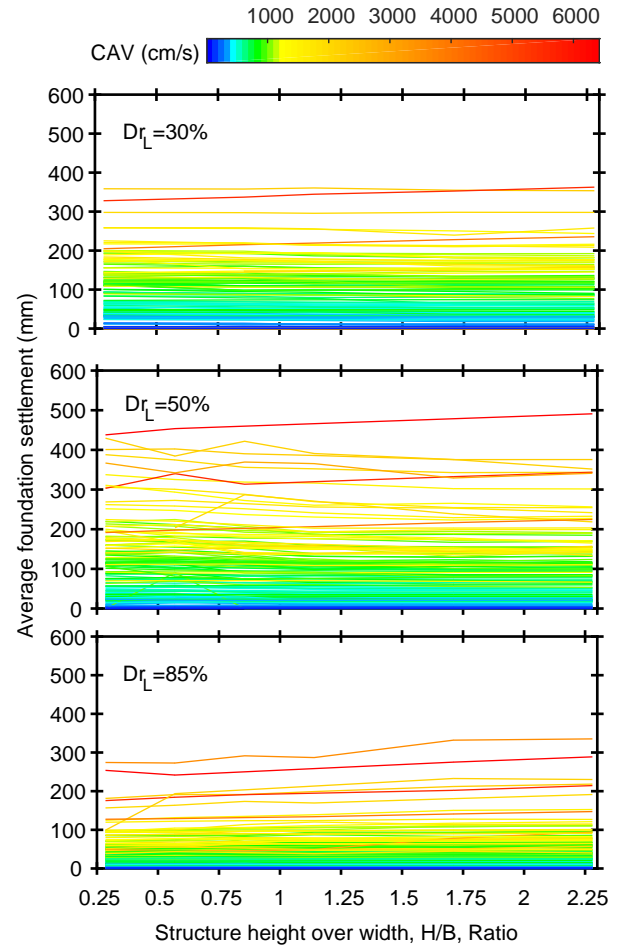


Figure 8. Influence of the structural height/width ratio on average permanent foundation settlements.

In summary, the most influential parameters considered in this study are the thickness and relative density of the liquefiable layer and the contact area and bearing pressure of the foundation. The  $H/B$  ratio of the structure is comparatively less influential in predicting

permanent settlement. Importantly, the influence and relative importance of each of these parameters is dependent on the intensity of the ground motion as well as the relative density of the underlying soil.

#### 4 CONCLUSIONS AND FUTURE RESEARCH DIRECTIONS

This study presents results from a numerical parametric study of SFS systems on layered liquefiable soil deposits. The main objective is to investigate the influence of excess pore pressure generation on soil-structure interaction effects and identify the main predictors of permanent foundation settlement. This is a necessary step before the development of mechanistically-sound, probabilistic predictive models of building settlement on liquefiable ground. Soil, structure, and ground motion characteristics are systematically varied to identify their effect, interdependence, and relative importance on the performance of the SFS system and in particular building permanent settlement.

Time-frequency analyses of the accelerations in the far-field and near-field compared to the base rock show that a major shift occurs in the frequency content of motions when significant excess pore pressures are generated. As extensive pore pressures develop, the soil stiffness reduces, which essentially filters the high frequency shear waves propagating through the soil column. Near the structure, since full liquefaction ( $r_u=1.0$ ) was often not predicted due to the higher confining pressure of the building, the transition in foundation accelerations to lower frequencies was less sharp (in time) than observed in the far-field where  $r_u=1.0$  was predicted. The rate and timing of cumulative foundation settlement is shown to be highly-correlated with the timing of excess pore pressure generation and strong shaking, after which settlement becomes negligible.

In general, the foundation settlement is shown to increase on looser liquefiable layers ( $D_{rL}=30$  to 50%), as expected. When this layer is dense ( $D_{rL}=85\%$ ), however, the foundation settlement remains considerable under moderate to strong ground motions, because of large shear-type deformations that can still be unacceptable. This consideration is particularly important when densification is used as a mitigation technique.

For loose to medium-dense liquefiable layers and under strong levels of shaking, foundation settlement is shown to increase when the thickness of this layer ( $H_L$ ) is increased up to approximately 8 to 10m. Further increases in  $H_L$  during stronger levels of shaking may result in greater strength loss and softening that would reduce the acceleration demand on the foundation, with a net effect being a slight reduction in total settlements.

The foundation contact pressure ( $q$ ) has a considerable influence on its settlement for all relative densities (e.g.,  $D_{rL}=30$ -85%), especially under strong levels of shaking. Increasing  $q$  from 30 to 160 kPa, for example, can amplify foundation settlement by approximately 60%.

Foundation contact area ( $A$ ) is also an influential parameter for strong levels of shaking, when its increase

can increase foundation settlements. However, at weaker levels of shaking, an opposite trend is observed.

Foundation settlement very slightly increased when increasing structure's height/width ratio ( $H/B$ ), without any increase in  $q$  or building mass. Importantly, the influence of these input parameters are shown to be highly interdependent.

#### 5 ACKNOWLEDGMENTS

This work was partly supported by the National Science Foundation (NSF) under Grant no. 1454431 and by the Department of Education through Grant no. P200A150042. Any opinions, findings, and conclusions or recommendations expressed in this material are those of the authors and do not necessarily reflect the views of the NSF or Department of Education. This work also utilized the Janus supercomputer, which is supported by the NSF (award number CNS-0821794) and the University of Colorado Boulder.

#### 6 REFERENCES

- Cubrinovski, M. and McCahon, I. 2012. Short term recovery project 7: CBD foundation damage, *Natural Hazards Research Platform*, Univ. of Canterbury, Christchurch, New Zealand.
- Dashti, S. and Bray, J.D. 2013. Numerical Simulation of Building Response on Liquefiable Sand, *J. Geotech. and Geoenv. Eng.*, ASCE, 139 (8): 1235-1249.
- Dashti, S., Bray, J. D., Pestana, J. M., Riemer, M. R., and Wilson, D. 2010a. Centrifuge testing to evaluate and mitigate liquefaction-induced building settlement mechanisms, *J. Geotech. Geoenviron. Eng.*, 136(7): 918-929.
- Dashti, S., Karimi, Z. 2017. Ground Motion Intensity Measures to Evaluate I: the Liquefaction Hazard in the Vicinity of Shallow-Founded Structures, *Earthquake Spectra*, EERI, 33(1): 241-276, DOI: 10.1193/103015EQS162M
- Elgamal, A., Yang, Z., and Parra, E. 2002. Computational modeling of cyclic mobility and post-liquefaction site response, *Soil Dynamics and Earthquake Engineering*, 22 (4): 259-271.
- Ishihara, K. and Yoshimine, M. 1992. Evaluation of settlements in sand deposits following liquefaction during earthquakes, *Soils Found.*, 32(1): 173-188.
- Karimi, Z. and Dashti, S. 2015a. Numerical Simulation of Earthquake Induced Soil Liquefaction: Validation against Centrifuge Experimental Results, *IFCEE2015*, ASCE, Geo-Institute, 11-20.
- Karimi, Z. and Dashti, S. 2015b. Numerical and Centrifuge Modeling of Seismic Soil-Foundation-Structure Interaction on Liquefiable Ground, *J. Geotech. Geoenviron. Eng.*, ASCE, 10.1061/(ASCE)GT.1943-5606.0001346 , 04015061.

- Karimi, Z. and Dashti, S. 2016a. Seismic Performance of Shallow Founded Structures on Liquefiable Ground: Validation of Numerical Simulations using Centrifuge Experiments, *J. Geotech. Geoenviron. Eng.* ASCE, 10.1061/(ASCE)GT.1943-5606.0001479.
- Karimi, Z. and Dashti, S. 2016b. Effects of Ground Motion Intensity Measures on Liquefaction Triggering and Settlement near Structures, *ICONHIC2016*, June 2016, Chania, Greece.
- Karimi, Z. and Dashti, S. 2017. Ground Motion Intensity Measures to Evaluate II: the Performance of Shallow-Founded Structures on Liquefiable Ground, *Earthquake Spectra*, EERI, 33(1): 277-298. DOI: 10.1193/103015EQS163M
- Karimi, Z., Dashti S., and Bullock, Z. (2017b). Influence of Soil and Structural Properties on the Response of Shallow-Founded Structures on Layered Liquefiable Deposits, *Geotechnical Frontiers 2017*, ASCE, Orlando, FL.
- Kramer, S. L., Sideras, S.S., and Greenfield, M.W. 2015. The Timing of Liquefaction and Its Utility in Liquefaction Hazard Evaluation, *6th International Conference on Earthquake Geotechnical Engineering*, Christchurch, New Zealand.
- Stockwell, RG, Mansinha, L, and Lowe, RP. 1996. Localization of the complex spectrum: the S transform, *IEEE Transactions on Signal Processing*, 44 (4): 998-1001.
- Tokimatsu, K. and Seed, H. B. 1987. Evaluation of settlements in sands due to earthquake shaking, *J. Geotech. Engrg.*, 113(8): 861-878.
- Yang, Z., Elgamal, A., and Parra, E. 2003. Computational model for cyclic mobility and associated shear deformation, *J. Geotech. Geoenviron. Eng.* ASCE, 129 (12): 1119-1127.
- Yang, Z., Lu, J., and Elgamal, A. 2008. *OpenSees Soil Models and Solid-Fluid Fully Coupled Elements: User's Manual*, Department of Structural Engineering, University of California, San Diego.
- Zhang, Y., Conte, J. P., Yang, Z., Elgamal, A., Bielak, J., and Acero, G., 2008. Two-dimensional nonlinear earthquake response analysis of a bridge-foundation-ground system, *Earthquake Spectra*, 24: 343–386.